Electronic Reconstruction at $SrMnO_3$-$LaMnO_3$ Superlattice Interfaces

Şerban Smadici,[1] Peter Abbamonte,[1] Anand Bhattacharya,[2] Xiaofang Zhai,[1] Bin Jiang,[1] Andrivo Rusydi,[3] James N. Eckstein,[1] Samuel D. Bader,[2] and Jian-Min Zuo[1]

[1]*Frederick Seitz Materials Research Laboratory, University of Illinois, Urbana, Illinois 61801, USA*
[2]*Center for Nanoscale Materials and Materials Science Division, Argonne National Laboratory, Argonne, Illinois 60439, USA*
[3]*Institute of Applied Physics, University of Hamburg, D-20355 Hamburg, Germany*

(Received 31 May 2007; published 9 November 2007)

We use resonant soft–x-ray scattering (RSXS) to study the electronic reconstruction at the interface between the Mott insulator $LaMnO_3$ and the band insulator $SrMnO_3$. Superlattices of these two insulators were shown previously to have both ferromagnetism and metallic tendencies [Koida *et al.*, Phys. Rev. B **66**, 144418 (2002)]. By studying a judiciously chosen superlattice reflection, we show that the interface density of states exhibits a pronounced peak at the Fermi level, similar to that predicted in related titanate superlattices by Okamoto *et al.* [Phys. Rev. B **70**, 241104(R) (2004)]. The intensity of this peak correlates with the conductivity and magnetization, suggesting it is the driver of metallic behavior. Our study demonstrates a general strategy for using RSXS to probe the electronic properties of heterostructure interfaces.

DOI: 10.1103/PhysRevLett.99.196404 PACS numbers: 71.45.Gm, 74.25.Jb, 78.70.Ck

The interface between two correlated electron systems may have properties that are qualitatively different from either of the two constituents, providing a potential route to new devices and physical properties [1]. An example is the interface between the d^1 Mott insulator $LaTiO_3$ (LTO) and the d^0 band insulator $SrTiO_3$ (STO), which experiments on superlattice heterostructures have suggested is metallic [2]. Dynamical mean field theory (DMFT) studies of this interface have suggested that the metallic behavior is driven by interfacial electronic reconstruction, characterized by the appearance of a quasiparticle peak at the Fermi level E_F in the density of states (DOS) of the interface layer [3,4]. Efforts to find this peak with angle-integrated photoemission studies of LTO-STO superlattices resulted in the observation of a small Fermi surface crossing [5]. However, a peak in the DOS clearly associated with the buried interface has not yet been observed.

Another example of a Mott-insulator–band-insulator interface is $LaMnO_3$-$SrMnO_3$. $LaMnO_3$ (LMO) is a Mott insulator with a $t_{2g}^3 e_g^1$ configuration while $SrMnO_3$ (SMO), which has a $t_{2g}^3 e_g^0$ configuration, can be considered a high-spin band insulator because its e_g shell is empty. Therefore, apart from the presence of the core t_{2g} spins, LMO-SMO is analogous to the LTO-STO system. A recent DMFT calculation predicted that the LMO-SMO interface should be a ferromagnetic metal, governed by double-exchange hopping of e_g electrons [6]. Large period LMO-SMO heterostructures synthesized previously were shown to have both ferromagnetism and metallic tendencies [7]; however, it is not clear whether this derives from electronic reconstruction at the interfaces.

In this Letter we present a study of LMO-SMO superlattices with resonant soft–x-ray scattering (RSXS). By judiciously choosing the thicknesses of the LMO and SMO sublayers, we obtained a structure whose third order superlattice reflection is directly sensitive to the DOS of the interface MnO_2 layer. We show that the DOS of the interface layer exhibits a quasiparticle resonance at E_F whose intensity correlates with the magnetization and conductivity of the overall structure. Our results confirm the predictions of Refs. [3,4] and demonstrate a general strategy for using RSXS to study the electronic structure of heterostructure interfaces.

Superlattices consisting of seven periods of $(8 \times \mathrm{LMO} + 4 \times \mathrm{SMO})$ and six periods of $(10 \times \mathrm{LMO} + 5 \times \mathrm{SMO})$ layers were grown on $SrTiO_3$ (STO) substrates by molecular beam epitaxy. The samples will be denoted $(\mathrm{LMO})_{2n}/(\mathrm{SMO})_n$ with $n = 4$ or $n = 5$ in the following. To avoid oxygen vacancies, which can cause anomalous metallic behavior through electron doping [8,9], the samples were both grown and postannealed in flowing ozone. Large amplitude reflection high-energy electron diffraction (RHEED) oscillations indicated two-dimensional epitaxial growth and scanning transmission electron microscopy (STEM) images showed well-defined superlattice interfaces [Fig. 1(b)]. The SMO and LMO overlayers in these structures are under $+2.8\%$ and -2.1% strain, respectively, which likely alters the exact pattern of orbital and magnetic order in the sublayers, but will not by itself induce metallic behavior [10,11]. X-ray reflectivity measurements showed clear interference fringes [Fig. 1(a)], indicating flat interfaces over macroscopic distances.

RSXS measurements were carried out at beam line X1B at the National Synchrotron Light Source in an ultrahigh vacuum diffractometer [12,13]. Measurements were done with the momentum transfer perpendicular to the plane of the heterostructure. We denote momenta in reciprocal units of the superlattice; i.e., Miller index L corresponds to a momentum $Q = 2\pi L/d$, where d is the superperiod. The incident light was polarized in the scattering plane (π polarization) with the channeltron detector integrating

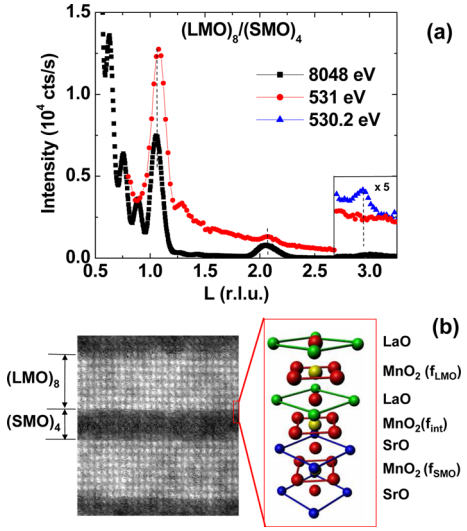

FIG. 1 (color online). (a) Specular x-ray scattering from the $n = 4$ superlattice with nonresonant hard–x-rays (squares), nonresonant soft–x-rays (circles), and soft x rays tuned close to the Fermi energy (triangles). Data are plotted on a linear scale to emphasize height differences between the peaks. (b) (left) STEM image of the $n = 4$ structure and (right) a drawing showing the interface region with scattering factors defined for the various atomic planes.

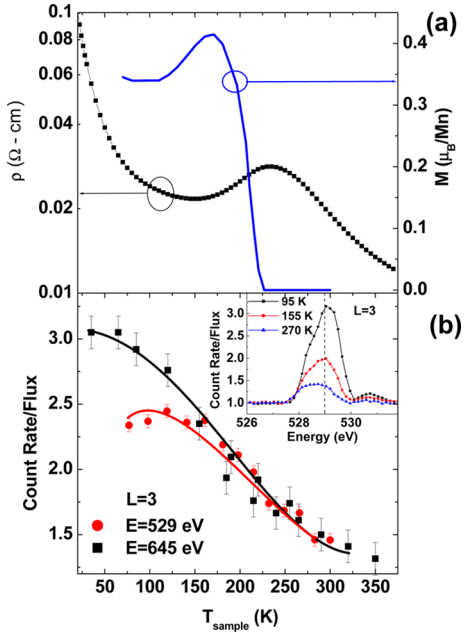

FIG. 2 (color online). (a) T dependence of the conductivity and magnetization of the $n = 4$ structure when cooled in 50 G [14]. (b) T dependence of the $L = 3$ reflection at O K and Mn L_3 edges and $L = 3$ for the $n = 4$ sample. Inset shows T dependent scans at O K edge.

over both final polarizations, i.e., both the $\pi \rightarrow \sigma$ and $\pi \rightarrow \pi$ scattering channels. Bulk sensitive RSXS measurements were performed at the Mn $L_{3,2}$ edges as well as the O K edge, which probes the $3d$ levels through hybridization, with the incident bandwidth set to 0.2 eV resolution.

Prior to RSXS studies the superlattices were characterized with x-ray absorption spectroscopy (XAS), resistivity, magnetization, hard–x-ray diffraction, and STEM. The STEM images were taken with a JEOL2010F field emission source microscope operated at 200 kV with a nominal 2.4 Å point resolution, $C_S = 1$ mm, and $C_C = 1.4$ mm. The resistivity of both samples exhibits a crossover to metallic behavior below $T_C \sim 225$ K [Fig. 2(a) and Ref. [14]]. At this temperature ferromagnetism also appears, with an average saturation magnetic moment at low temperatures of $1.75\mu_B$/Mn and $1.4\mu_B$/Mn for the $n = 4$ and $n = 5$ samples, respectively. This behavior is consistent with double-exchange ferromagnetism as observed in previous studies [7,14]. Because both LMO and SMO are insulating and antiferromagnetic (A- and G-type, respectively [15]), it seems likely, though this has not been proven, that magnetism originates at the interfaces. XAS measurements were done in electron yield mode probing only the top ~20 Å layer of the sample [16], which is an LMO layer. The first buried interface contributed <5% to the spectra [Figs. 3(b) and 4(a); note the location of E_F], which closely resemble past studies of LMO powders [17] indicating good surface quality.

In Fig. 1 we show hard–x-ray diffraction data for the $n = 4$ superlattice. Thickness oscillations are visible, as well as several superlattice reflections residing at integer values of L. A key observation is that the $L = 3$ reflection is suppressed [18]. This is expected by symmetry. For a superlattice with sublayer indices m and n, the structure factor will vanish for any reflection $L = u + v$ where u and v are integers and $u/v = m/n$. For the specific case of the $n = 4$ superlattice the structure factor for the $L = 3$ reflection is

$$S(L = 3) = 2f_{\text{int}} - f_{\text{LMO}} - f_{\text{SMO}}, \qquad (1)$$

where f_{LMO} and f_{SMO} are the scattering factors of the MnO_2 planes of the LMO and SMO layers, respectively, and f_{int} is the scattering factor for the MnO_2 plane at the interface (Fig. 1) [19]. Notice that the form factors for the LaO and SrO layers do not contribute. The $L = 3$ reflection is forbidden by symmetry as long as the interface MnO_2 form factor is the average of the form factors of MnO_2 planes of the LMO and SMO layers. The intensity of this reflection is therefore a measure of the degree to which the mirror symmetry of the interface is broken. That this reflection is weak in hard–x-ray diffraction is an indication that the interfaces are sharp, with the symmetric form of Eq. (1) not disrupted by interdiffusion or other interface reconstructions.

Results of resonant scattering studies, which probe the unoccupied DOS, reveal something surprising [Fig. 1(a)]. If the photon energy is tuned above the O K threshold—to a nonresonant condition—an L scan reveals that the $L = 3$ is extinguished, in agreement with hard–x-ray measurements. However, if the energy is tuned at 530.2 eV, near the Fermi onset, the $L = 3$ becomes visible. Evidently the

symmetry of the LMO-SMO interface, while preserved by the atomic lattice, is broken electronically near the Fermi energy. This is evidence that the interfaces are electronically reconstructed.

Our primary observation is the energy dependence of the $L = 3$ reflection near the O K edge, shown in Fig. 3. This figure, which compares the intensity of the $L = 3$ reflection to an XAS spectrum of the LMO top layer, shows which part of the unoccupied DOS is reconstructed. The $L = 3$ reflection has maximum intensity at the edge onset, where RSXS probes states at the Fermi level. In addition, weaker peaks are visible at 531.5 eV and 534 eV, which coincide roughly with the Mn $e_{g,\uparrow}$ and $e_{g,\downarrow}$ bulk bands of LMO. In contrast, both the $L = 1$ and $L = 2$ reflections in Fig. 3 have a large nonresonant component below the absorption edge and strong peaks from bulk states above the edge. The resonant enhancement at E_F also occurs for $L = 1$ and $L = 2$ scattering since f_{int} enters the expressions for $S(L = 1)$ and $S(L = 2)$. We conclude that electronic reconstruction of the LMO-SMO interface occurs primarily near E_F, although higher energies clearly participate to a lesser degree.

We propose that the main resonance observed at 529 eV corresponds to a quasiparticle peak at E_F, as predicted for a Mott-band-insulator interface [3]. A connection to the DMFT calculations for LTO-STO superlattices in Ref. [3] can be made by noting that, in the absence of nonresonant scattering and excitonic effects, $\mathrm{Im}[f_{int}]$ should be proportional to the interface spectral function $A_{int}(\omega)$. It was shown in Ref. [3] that $A_{int}(\omega)$ has a strong peak at E_F, as we observe here [20]. The weaker features at higher energy indicate interface hybridization of excitations involving crystal field and Jahn-Teller effects, as well as Hubbard and Hund's rule interactions. To account for these features quantitatively would require microscopic modeling coupled with Kramers-Kronig analysis.

The connection between the $L = 3$ resonance at E_F and metallic behavior is also supported by its T dependence, shown in Fig. 2(b). As T is lowered, the intensity of the E_F resonance rises, the inflection point coinciding with the peak in the resistivity and the onset of an in-plane magnetic moment [14] [Fig. 2(a)]. This is evidence that the resonance is closely related to metallic tendencies and that the magnetism and metallic conduction both arise from reconstruction of interfaces as considered by Okamoto *et al.* [3,4]. Interestingly, the E_F peak also appears to be composed of two features separated by 0.75 eV.

In order to study the magnetism of the superlattice, we also measured the $L = 3$ reflection at the Mn $L_{3,2}$ edges. Previous RSXS studies [21–25] of manganite systems have shown that both orbital and magnetic order can contribute to scattering at these edges. In our structures, in addition to magnetic order, one expects an interesting participation of the e_g orbital degree of freedom. In the SMO layer the $d_{x^2-y^2}$ orbital should be lower in energy than the $d_{3z^2-r^2}$

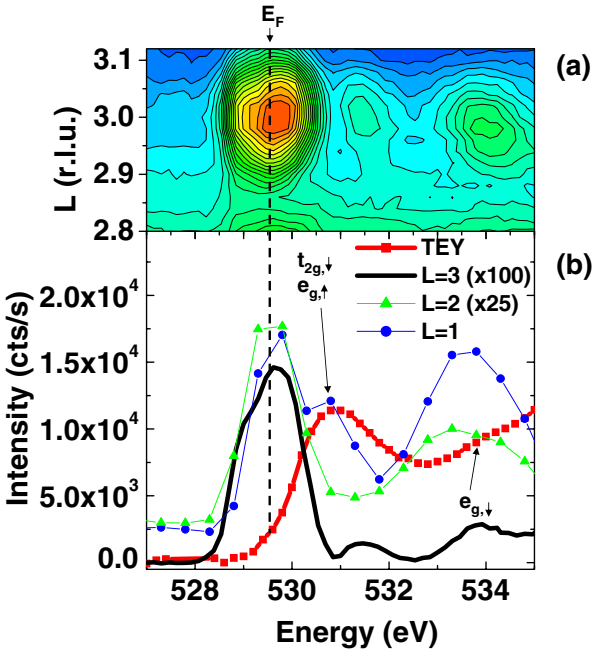

FIG. 3 (color online). (a) Resonance profile at $L = 3$ and O K edge for the $n = 4$ sample. The strongest resonance is at E_F and $L = 3$. (b) Scattering at $L = 3$ and $T = 90$ K (line), at $L = 1$ (circles), and $L = 2$ (triangles), compared to XAS data (squares, aligned to zero below the edge). Notice that the thickness of this superlattice is 32.5 nm, which is much smaller than the penetration depth of soft–x-rays ~100 nm—self-absorption effects are estimated to be ~10%. The strong resonant enhancement before the O K edge is indicative of an electronic effect. The peaks at higher energy are aligned with features in the absorption spectra, as assigned in Ref. [17].

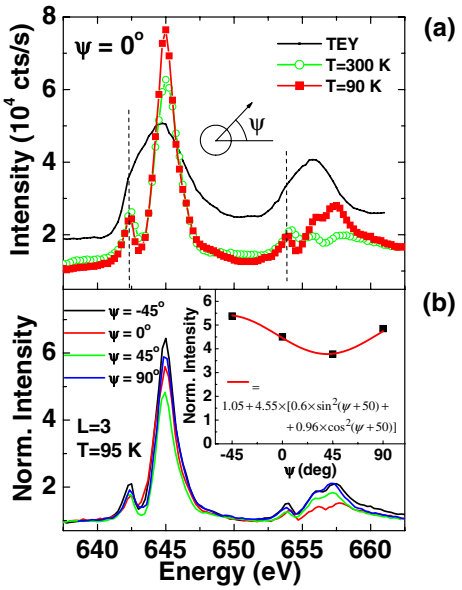

FIG. 4 (color online). (a) Energy profiles near Mn $L_{3,2}$ edges at $L = 3$ for two temperatures (squares and circles) and sample absorption measured by electron yield (line). (b) $L = 3$ scattering at 645 eV for a few azimuthal orientations. Inset: the measured azimuthal dependence and a fit curve.

orbital (z is along the c axis). The situation is reversed in LMO, and one therefore expects the total structure to have a modulation in the orbital occupancy with the superlattice period. This is in addition to the Jahn-Teller effect that may still play a role in the LMO layers despite the presence of strain [10,11]. Separating charge, orbital, and magnetic scattering at the Mn L edge can be done using the azimuthal ψ dependence. The magnetic scattering is proportional to $(\hat{\boldsymbol{\epsilon}}_f^* \times \hat{\boldsymbol{\epsilon}}_i) \cdot \mathbf{S}$, where $\hat{\boldsymbol{\epsilon}}_i$ and $\hat{\boldsymbol{\epsilon}}_f$ are the incident and final polarizations, respectively, and $\mathbf{S}$ is the local spin. For our experimental geometry, this simplifies to

$$I \propto \cos^2(\theta)\sin^2(\psi) + \sin^2(2\theta)\cos^2(\psi), \qquad (2)$$

where θ is the angle of incidence on the sample. In contrast, the strain-induced orbital scattering should be independent of ψ since strain does not break the tetragonal symmetry of the unit cell. Good agreement is obtained between our measurements at four ψ values and Eq. (2) [Fig. 4(b), inset] with a magnetic moment at $\sim 50°$ between the a and b axes and a constant offset equal to the off-resonance background. This suggests that the scattering is primarily magnetic [26].

The T dependence at the Mn L edge [Fig. 2(b)] closely follows that observed at the O K edge. This again suggests that the E_F resonance and the interfacial magnetization are related. The overall picture that emerges is that the reconstructed interfaces exhibit the same connection between charge carrier itineracy and magnetic order familiar from bulk colossal magnetoresistance materials. As the temperature is lowered, ferromagnetism nucleates, increasing the mobility and therefore the spectral weight at E_F. An open question is the nature of the resistive rise for $T < 100$ K [Fig. 2(a)]. This rise might signify the emergence of an ordered state.

We note that our O K edge measurements [Fig. 3(b)] closely resemble those of a recent RSXS study of bulk magnetite interpreted as a DOS modulation near E_F and the presence of charge order [27]. Our results, which also show a DOS modulation, indicate the presence of reconstructed interfaces [Eq. (1)]. There is no contradiction between these interpretations.

In conclusion, we have used RSXS to investigate superlattices of the Mott insulator $LaMnO_3$ and the "band" insulator $SrMnO_3$. By choosing a specific combination of superlattice reflection and layer periods, we were able to isolate the electronic properties of the interface. We show that the interfacial DOS exhibits a peak at E_F as shown in the calculations of Okamoto *et al.,* suggesting that ferromagnetism and metallic behavior in this system arise from electronic reconstruction of the interfaces. Our study demonstrates a general strategy for using RSXS to probe the electronic properties of interfaces.

The authors acknowledge helpful discussions with John Freeland and C.-C. Kao. This work was supported by the Office of Basic Energy Sciences at the U.S. Department of Energy. Resonant scattering experiments were supported under Grant No. DE-FG02-06ER46285 and digital synthesis work under Grant No. DE-AC02-06CH11357, Subcontract No. WO 4J-00181-0004A. The work at Argonne was supported under Contract No. DE-AC02-06CH11357 and the use of the NSLS under Contract No. DE-AC02-98CH10886.

[1] C. H. Ahn *et al.*, Rev. Mod. Phys. **78**, 1185 (2006).
[2] A. Ohtomo, D. A. Muller, J. L. Grazul, and H. Y. Hwang, Nature (London) **419**, 378 (2002).
[3] S. Okamoto and A. J. Millis, Phys. Rev. B **70**, 241104(R) (2004).
[4] S. Okamoto and A. J. Millis, arXiv:cond.-matt.0507150.
[5] M. Takizawa *et al.*, Phys. Rev. Lett. **97**, 057601 (2006).
[6] C. Lin, S. Okamoto, and A. J. Millis, Phys. Rev. B **73**, 041104(R) (2006).
[7] T. Koida, M. Lippmaa, T. Fukumura, K. Itaka, Y. Matsumoto, M. Kawasaki, and H. Koinuma, Phys. Rev. B **66**, 144418 (2002).
[8] G. Herranz *et al.*, arXiv:0704.2523.
[9] D. A. Muller, N. Nakagawa, A. Ohtomo, J. L. Gazul, and H. Y. Hwang, Nature (London) **430**, 657 (2004).
[10] Y. Wakabayashi *et al.*, Phys. Rev. Lett. **96**, 017202 (2006).
[11] K. H. Ahn and A. J. Millis, Phys. Rev. B **64**, 115103 (2001).
[12] P. Abbamonte, L. Venema, A. Rusydi, I. Bozovic, G. Logvenov, and G. A. Sawatzky, Science **297**, 581 (2002).
[13] P. Abbamonte, A. Rusydi, Ş. Smadici, G. D. Gu, G. A. Sawatzky, and D. L. Feng, Nature Phys. **1**, 155 (2005).
[14] A. Bhattacharya, X. Zhai, M. Warusawithana, J. N. Eckstein, and S. D. Bader, Appl. Phys. Lett. **90**, 222503 (2007).
[15] E. O. Wollan and W. C. Koehler, Phys. Rev. **100**, 545 (1955).
[16] M. Abbate *et al.*, Surf. Interface Anal. **18**, 65 (1992).
[17] M. Abbate *et al.*, Phys. Rev. B **46**, 4511 (1992).
[18] The residual scattering at $L = 3$ seen using hard x rays (Fig. 1) is due to a small ($\sim 10\%$) number of growth defects [e.g., $(LMO)_7/(SMO)_5$] in the $(LMO)_8/(SMO)_4$ sample.
[19] The atomic scattering factors are tensors, i.e., $f = f^{i,j}$. For notational simplicity, however, we leave off the indices in our discussion.
[20] See EPAPS Document No. E-PRLTAO-99-001746 for a superlattice that has inbuilt interface symmetry breaking. For more information on EPAPS, see http://www.aip.org/pubservs/epaps.html.
[21] K. J. Thomas *et al.*, Phys. Rev. Lett. **92**, 237204 (2004).
[22] S. S. Dhesi *et al.*, Phys. Rev. Lett. **92**, 056403 (2004).
[23] S. B. Wilkins *et al.*, J. Phys. Condens. Matter **18**, L323 (2006).
[24] U. Staub *et al.*, Phys. Rev. B **71**, 214421 (2005).
[25] J. Okamoto *et al.*, Phys. Rev. Lett. **98**, 157202 (2007).
[26] Recent polarized neutron reflectivity measurements have detected a modulated magnetic structure in a LMO-SMO superlattice at low temperatures; see S. J. May *et al.*, arXiv:0709.1715, and A. Bhattacharya *et al.*, arXiv:0710.1452.
[27] D. J. Huang *et al.*, Phys. Rev. Lett. **96**, 096401 (2006).